Sādhanā Vol. 41, No. 3, March 2016, pp. 369–376

Energy and exergy analysis in double-pass solar air heater

P VELMURUGAN* and R KALAIVANAN

Department of Mechanical Engineering, Annamalai University, Annamalai Nagar 608002, Tamilnadu, India
e-mail: pvsrlme@gmail.com

MS received 14 October 2014; revised 16 August 2015; accepted 30 October 2015

Abstract. In this study, an attempt is made to improve the energy and exergy performance of solar air heater by employing double pass with different absorber surface geometries (roughened, finned, and v-corrugated wire mesh) in the second pass, and also by mounting longitudinal fins in the back side of the absorber plate (first pass). The effect of varied mass flow rate and solar intensity on temperature rise of air, energy efficiency, exergy gain and pressure drop at steady state condition was determined for different types of solar air heaters utilizing an indoor solar simulator. The temperature rise of air, thermal efficiency and exergy gain depends on mass flow rate, surface geometries of absorber and solar intensity, whereas the pressure drop depends on mass flow rate and surface geometries of absorber.

Keywords. Solar air heater; double pass; roughened; finned; wire mesh; energy; exergy.

1. Introduction

Solar energy can play vital role in clean and sustainable energy sources. Solar air heaters have an important place among application of solar energy system. The efficiency of solar air heater is low, as air has worse thermodynamic properties in terms of heat transfer from absorber plate to flowing air. The convective heat transfer between absorber plate and air is enhanced by creating turbulent flow or modifying the absorber surface shape. The absorber surface shape is influential in the design of solar air heater. The main applications for solar air heaters are space heating, drying and paint spraying operations.

Numerous solar air heating devices have been developed and used experimentally. The effects of materials and construction of the absorber upon the energy and exergy performance of the solar air heaters were also reported in the literature widely. Sopian *et al* [1] conducted indoor experiments with varied mass flow rate (0.03–0.07 kg/s) and solar intensity (480–550 W/m^2) on a counter flow solar air heater with and without steel wool as porous media in the second channel. Several combinations of upper (3.5–10.5 cm) and lower channel (7–14 cm) depths were considered for the thermal performance investigation. The thermal performance of a double glass double pass solar air heater under varied mass flow rate (0.015–0.14 kg/s) with a packed bed above the absorber plate was investigated by Ramadan *et al* [2] who concluded that the thermal efficiency is insignificant beyond a mass flow rate of 0.05 kg/s. The performance of single and double pass solar air heater with fins and steel wire mesh as absorber is investigated experimentally by Omojaro & Aldabbagh [3] who found that the efficiency of the double pass is higher than the single pass by 7–19.4% in the mass flow rate range of 0.012 kg/s and 0.038 kg/s. Double glass double flow finned and v-corrugated plate solar air heater was investigated theoretically and experimentally by El-Sebaii *et al* [4]. The results showed that the double pass v-corrugated plate solar air heater was 9.3–11.9% more efficient compared to the double flow finned plate solar air heater. Ozgen *et al* [5] experimentally investigated the thermal performance of double flow solar air heater by inserting an absorber plate made of aluminium cans. Karsli [6] determined the first and second law efficiencies for four types of flat plate solar air heaters. The results showed that the efficiency depends on the solar radiation and the construction of solar air heaters. Gupta & Kaushik [7] studied the energetic performance of flat plate solar air heater to establish the optimal performance parameters for maximum exergy delivery during the collection of solar energy. They stated that based on the output energy evaluation, the solar air heater should have high aspect ratio, low duct depth and low inlet temperature of air. They have observed and proved that if the inlet temperature of air is low, then maximum exergy output is achieved at lower mass flow rate. Esen [8] reported an experimental study to evaluate the energetic and exergetic efficiencies of four types of double flow solar air heaters with several obstacles and without obstacles under a wide range of operating conditions. Akpinar & Koçyiğit [9] performed an experimental study to investigate the performance

*For correspondence

of four flat plate solar air heater. Three of them were several obstacles and the other one was without obstacles at two different air mass flow rates (0.0052 kg/s and 0.0074 kg/s). The first and second laws of efficiencies were determined for solar air heaters and comparisons were made among them.

Though several works were carried out by earlier researchers, it is observed that experimental attempts to improve the energy and exergy performance of solar air heater is limited and is attempted in this study. In addition, novel designs not reported viz., roughened plate double pass with longitudinal fins, finned plate double pass with longitudinal fins and v-corrugated wire mesh double pass with longitudinal fins were developed and tested in an indoor testing facility. The temperature rise of air, energy efficiency, exergy gain and pressure drop were determined at varied solar intensities and mass flow rates for the attempted solar air heaters and compared with conventional solar air heater.

2. Experimental set-up and procedure

The top plane of the collector (glass cover) is uniformly heated by an incident radiation using solar simulator. An indoor solar simulator test facility photographically shown in figure 1 uses 20 halogen lamps, each with a rated power of 300 W. The lamps are fixed on a frame having similar area of the collector, placed 1 m above the glass cover such that the maximum average radiation of 645 W/m^2 can be reached at full load conditions. During experimentation, incident radiation was adjusted by the input power to the lamps, being controlled by two AC variacs (4.5 kW each). The incident radiation was measured at the surface of the glass cover by using solarimeter (KIMO SL-100) calibrated using standard pyranometer. The average value of the incident radiation on the collector top plane was determined as follows. The plain glass cover was divided into 20 sectors, and the measurement of the incident radiation was performed at each sector separately corresponding to input power to the lamps. The deviation of individual sectors measured values from that of the overall average values ranges from -4.72% to 4.04%. This error range is within the allowable deviation of the indoor tests for solar collector performance standards [10, 11], which indicates that a deviation up to $\pm 10\%$ is acceptable.

Four different solar air heaters are used. The main features of the four tested solar air heaters are described below. The air flow is provided as seen in figure 2(a–d). Type-A is named as v-corrugated wire mesh double pass solar air heater with longitudinal fins (figure 2a). V-corrugated wire mesh absorber surface fabricated with 0.3 mm diameter steel wire mesh consists of 2.5 mm $\times$ 2.5 mm in cross-sectional opening. Single layer wire mesh painted with black is assembled in a transverse v-corrugated shape whose angle and height are 60° and 2.5 cm respectively and also 17 longitudinal fins are mounted in the back side of absorber plate. Type-B is named as finned plate double pass solar air heater with longitudinal fins (figure 2b). Finned absorber surface is fabricated with 17 longitudinal fins made of mild steel whose dimensions are 1.98 m 0.025 m and 0.001 m (length, height and thickness) respectively, whereas 17 longitudinal fins are also mounted in the back side of absorber plate. Type-C is named as roughened plate double pass solar air heater with longitudinal fins (figure 2c). Roughened absorber surface was fabricated with a mild steel wire of diameter (e) 1.5 mm and pitch (p) 15 mm. Prasad [12] optimized the relative roughness pitch (p/e) and relative roughness height (e/D_h) for solar air heater as 10 and 0.0316 respectively and these parametric values are employed in this study. In addition, 17 longitudinal fins are provided in the back side of the absorber plate. Type-D is the conventional single pass flat plate solar air heater (figure 2d). In single pass solar air heater, air

Figure 1. Photographic view of experimental setup.

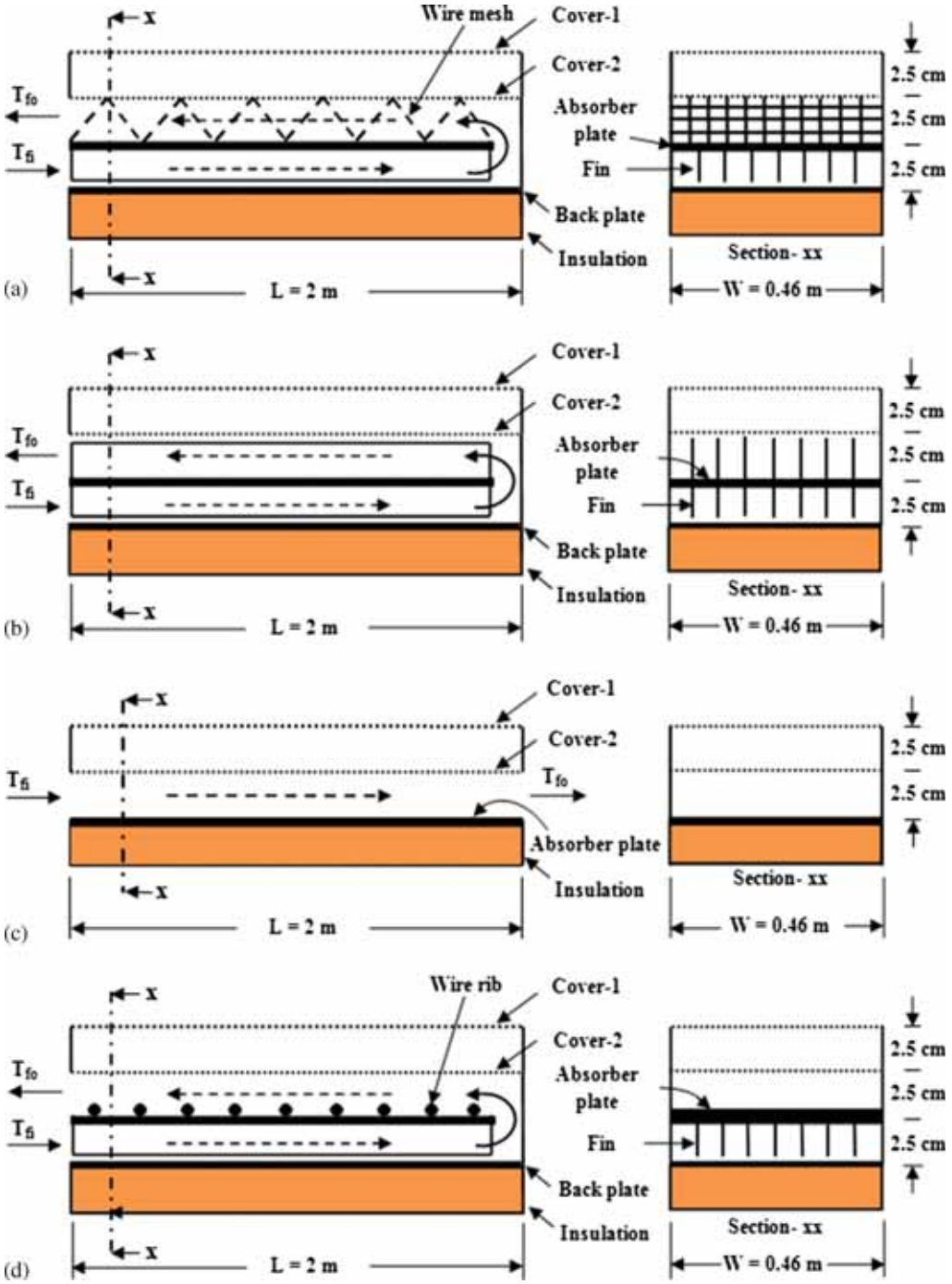

Figure 2. Various configuration of solar air heaters: (**a**) V-corrugated wire mesh double pass solar air heater with longitudinal fins (type-A), (**b**) Finned plate double pass solar air heater with longitudinal fins (type-B), (**c**) Roughened plate double pass solar air heater with longitudinal fins (type-C), (**d**) Conventional flat plate single pass solar air heater (type-D).

passes between absorber plate and cover-2, whereas in double pass solar air heater, air passes between back plate and absorber plate and then flows between the absorber plate and cover-2. The solar air heaters consist of the two glass covers, absorber plate, back plate and an insulated container. Low-iron glass (4 mm thickness) was used as glazing and the absorbers were constructed using mild steel coated with black paint. The dimensions of all the solar air heater absorber plates were maintained as 2 m 0.46 m and 1 mm (length, width and thickness respectively). The depth of each flow channel of solar air heater is 2.5 cm and covered with thermocole to curtail the losses to the ambience.

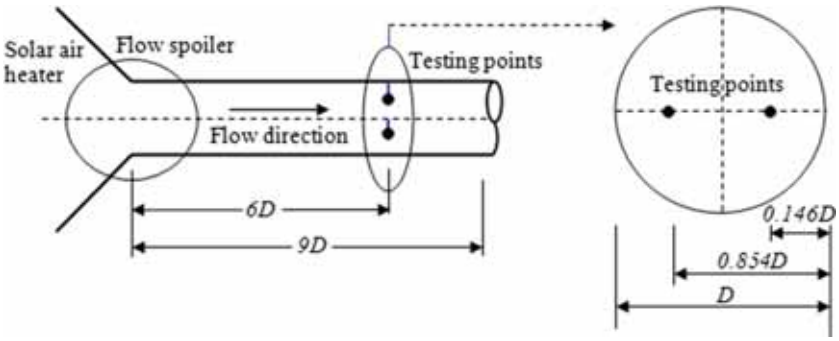

Figure 3. Air velocity measurement locations and testing points.

A variable speed centrifugal blower, capable of delivering a 180 m^3/h is employed to suck the air through the solar air heater. The mass flow rate was controlled by varying the blower speed using AC variac (1.5 kW). The air mass flow rate inside the solar air heater is calculated from air velocity, measured by a hot wire anemometer (KIMO VT-100) at the solar air heater outlet, for a known cross-sectional area of the pipe. Air velocity measuring points is located in the pipe (7.5 cm diameter, 80 cm long) between solar air heater exit section and blower. Figure 3 shows the distance between testing points (measuring points) and flow spoiler (e.g., converging section, valve and elbow) must be six times of pipe diameter (6D) along the flow direction, meanwhile the whole length of the straight, non-spoiler pipe was maintained more than 9D to eliminate the vortex impact. As suggested by Yang *et al* [13], two additional testing points are provided in the cross-sectional area to obtain the average value of air flow velocity distribution in the pipe. Forced convection was created around the solar air heater with a velocity of 1.5 m/s by an electrical fan (60 W). The vane type anemometer (AN 100) was used to measure air velocity around the solar air heater. The calibrated copper-constantan thermocouples (T-type) were used to measure the temperatures at six points along x-axis (flow direction of air) of the absorber plate, three points each in upper and lower glass covers along x-axis, three points distributed over the back plate along x-axis. Apart from the above locations, thermocouples were fixed at the inlet and exit section (3 points each-transverse direction of air flow) to measure the inlet and outlet air temperatures. The pressure drop across the solar air heater was measured by digital manometer (HT-1891). The steady state inlet, outlet air and absorber plate temperatures were noted The mass flow rate and solar intensity of solar air heater were varied from 0.01 to 0.04 kg/s and 500 to 600 W/m^2 respectively, and the results are reported.

3. Energy and exergy analysis

The useful energy gain (Q_f) by the working fluid is calculated from the following equation [14]

$$Q_f = mc_p\left(T_{fo} - T_{fi}\right). \tag{1}$$

Energy efficiency (η) of the heater is obtained from

$$\eta = Q_f / A_c I. \tag{2}$$

The exergy gain is defined as the increase of exergy, in the flow of fluid while passing through the solar air heater. Neglecting changes of kinetic and potential energy, and treating air as perfect gas, the exergy gain (Ex), considering pressure drop based on the second law of thermodynamics as [15]

$$Ex = mc_p\left(T_{fo} - T_{fi} - T_a \ln\left(T_{fo}/T_{fi}\right)\right) - (m/\rho)\,\Delta P\left(T_a/T_{fm}\right). \tag{3}$$

4. Uncertainty analysis

The error in a measurement is usually defined as the difference between its true value and the measured value and the term uncertainty is used to refer to a possible value that may include an error. Uncertainty analysis (the analysis of uncertainties in experimental measurement and results) is a powerful tool, particularly when it is used in the planning and design of experiments.

The result R is a given function in terms of the independent variable. Let W_R be the uncertainty in the result and $W_1, W_2, \ldots, W_n$ be the uncertainties in the independent variable. The result R is a given function of the independent variables $X_1, X_2, \ldots, X_n$. If the uncertainties in the independent variables are all given with same odds, then uncertainty in the result having these odds is calculated by [16]

$$W_R = \left[\left(\frac{\partial R}{\partial X_1}W_1\right)^2 + \left(\frac{\partial R}{\partial X_2}W_2\right)^2 + \ldots + \left(\frac{\partial R}{\partial X_n}W_n\right)^2\right]^{1/2}. \tag{4}$$

The independent parameters measured in the experiments reported here are air inlet and outlet temperatures, air velocity, pressure in the flow channel and solar radiation. To carry out these experiments, T-type thermocouple with accuracy 0.1°C, hot wire anemometer with ±3% accuracy, digital manometer with ±0.3% and solarimeter with 1% accuracy were used.

The total uncertainty in determining mass flow rate and energy efficiency was estimated by Eq. (4). Calculations show that the total uncertainty in mass flow rate and energy efficiency is ±3.18% and ±3.55%, respectively.

5. Results and discussion

Two independent sets of experiments at constant wind velocity (1.5 m/s) around the solar air heater were conducted to investigate the energy and exergy performance of type-A, type-B, type-C and type-D solar air heaters. In the first set the mass flow rate is varied inside the solar air heater (0.01–0.04 kg/s) at constant solar intensity (600 W/m^2). In the second set of experiments the solar intensity is varied between 500 and 600 W/m^2 by keeping constant mass flow rate (0.04 kg/s).

5.1 *Effect of varied mass flow rate*

As seen from figure 4, the temperature rise of air decreases with increasing mass flow rate for all four configurations as reported by Karim & Hawlader [17]. According to figure 4, the temperature rise of air is maximum at lower mass flow rate (0.01 kg/s), and minimum at higher mass flow rate (0.04 kg/s) for all solar air heaters attempted. This behaviour is explained by longer constant times of air with the hot surfaces inside the solar air heater. In addition, the temperature rise of air for type-A solar air heater (both enhanced turbulence and more heat transfer area) is higher than that of type-B solar air heater (enhanced more heat transfer area), than that of type-C solar air heater (enhanced turbulence and medium heat transfer area) and also that of type-D solar air heater (without enhanced turbulence and heat transfer area). Omojaro & Aldabbagh [3] conducted similar experiment and reported a rise in air temperature of 17°C (m = 0.012 kg/s, I = 600 W/m^2), while El-khawajah *et al* [19] reported a rise of 21.5°C (m = 0.0121 kg/s, I = 600 W/m^2) air temperature. In the present investigation the rise in air temperature was recorded as 26.28°C a mass flow rate of 0.01 kg/s and solar intensity of 600 W/m^2 for type-A, which is higher by 34.31% and 18.18% than the earlier results reported. Increased turbulence and heat transfer area by introduction of wire mesh and fins in double-pass might contribute to the higher value.

Figure 5 presents the energy efficiency for type-A, type-B, type-C and type-D solar air heaters at mass flow rate ranging from 0.01 to 0.04 kg/s. It can be seen from figure 5 that the energy efficiencies of all solar air heaters increase with mass flow rate. This is because the heat removal capacity depends directly on the mass flow rate. According to figure 5, maximum efficiencies were 82.29% in type-A, 71.37% in type-B, 67.73% in type-C and 53.60% in type-D for a mass flow rate of 0.04 kg/s. The efficiency of solar air heater increased approximately 1.5-fold in type-A, 1.3-fold in type-B and 1.2-fold in type-C compared to the type-D conventional solar air heater. Moreover, the energy efficiency of double pass solar air heaters (type-A, type-B and type-C) are higher than that of conventional single pass solar air heater (type-D) due to the enhanced path length and introduction of longitudinal fins which reduces the absorber plate temperature and consequently, minimizes the heat losses to the ambient. Mohamad [18] opined that an increase in the temperature of the absorber plate increases the heat losses by radiation and convection to ambience. Experimental results proved that type-A is 15.68–28.69% more efficient than type-D, 9.18–14.56% more efficient than type-C and 4.88–10.92% more efficient than type-B for the attempted conditions. Further, the introduction of wire mesh (type-A) increases the effective heat transfer area per unit volume of packed (wire mesh) duct, and therefore, the volumetric heat transfer coefficient between the wire mesh and flowing air increases to result in higher energy efficiency. Another reason for enhancement of its energy performance

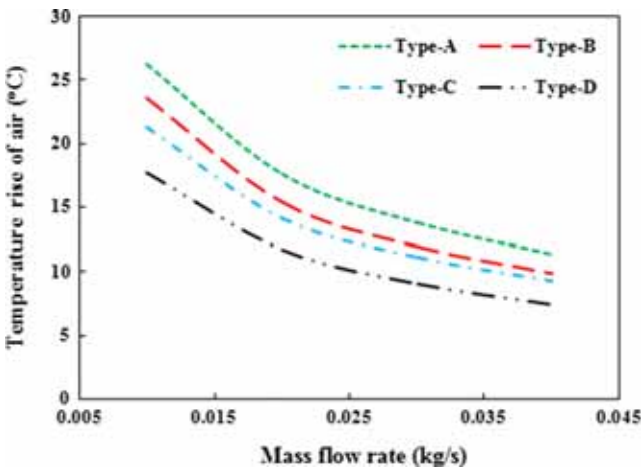

Figure 4. Variation of temperature rise of air with mass flow rate of air.

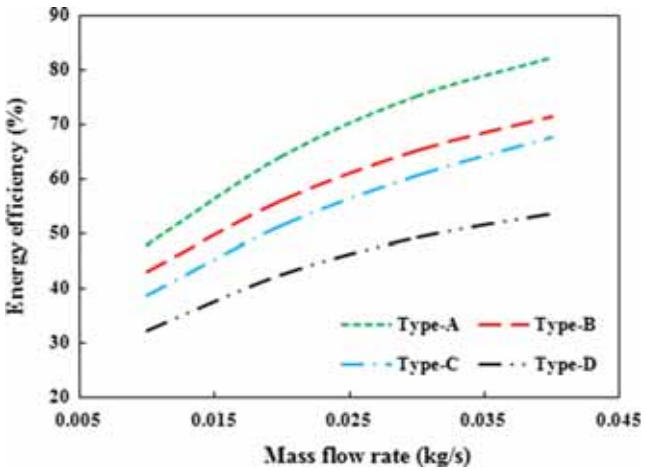

Figure 5. Variation of energy efficiency with mass flow rate of air.

is due to the fact that in case of packed (wire mesh) solar air heater, solar radiation are progressively absorbed by the layer of wire mesh and the remaining radiations are absorbed by the absorber plate. Thus not only the absorber plate but the wire mesh also works as the absorber of solar radiation. Therefore, the heat energy due to absorption of solar radiation is distributed throughout the wire mesh and the absorber plate and dissipated more effectively to the flowing fluid due to very large surface area being in contact with the flowing fluid in a packed (wire mesh) solar air heater as compared to type-B, type-C and type-D solar air heaters. During their investigation, Omojaro & Aldabbagh [3] conducted experiments by a double-pass solar air heater with wire mesh and longitudinal fins fitted in the second channel. They conducted experiments at $m = 0.038$ kg/s and $I = 600$ W/m^2. Omojaro and Aldabbagh further reported a maximum energy efficiency of 63.74%. For an identical solar radiation intensity and flow rate of 0.042 kg/s, El-khawajah *et al* [19] achieved a maximum efficiency of 79.5%. Further, Prasad *et al* [20] reported an efficiency of 68.5% while using a double cover glazing in a single-pass solar air heater with wire mesh ($m = 0.0347$ kg/s). Dhiman *et al* [21] investigated counter and parallel flow packed bed solar air heaters ($m = 0.0386$ kg/s) reported 73% efficiency. In this study maximum experimental energy efficiency of 82.29% is obtained at a mass flow rate of 0.04 kg/s and radiation intensity of 600 W/m^2 for Type-A.

The exergy gain against mass flow rate for type-A, type-B, type-C and type-D solar air heaters is shown in figure 6. The exergy gain decreases with increase in mass flow rate for type-A, type-B, type-C and type-D due to minimal increase in air temperature and is consistent with Sun *et al* [15]. It is observed from figure 6 that the minimum and maximum exergy gain through the four types solar air heaters (type-A, type-B, type-C and type-D) was 54.08, 43.35, 39.42 and 25.46 W for 0.04 kg/s and 63.15, 53, 45.2 and 32.27 W for 0.01 kg/s, respectively. Gupta & Kaushik [7] proved that maximum exergy gain is achieved at lower mass flow rate.

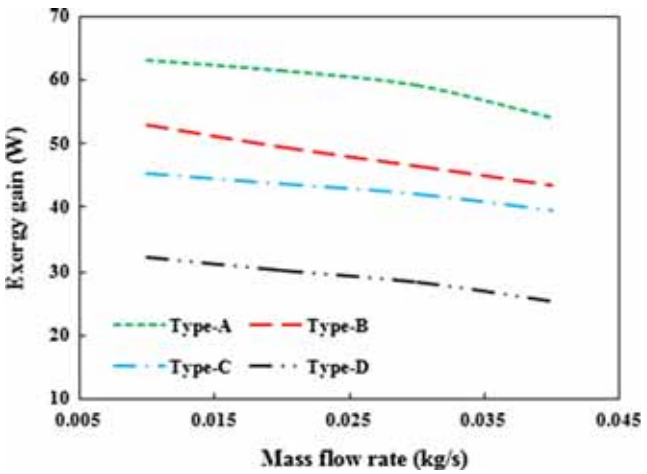

Figure 6. Variation of exergy gain with mass flow rate of air.

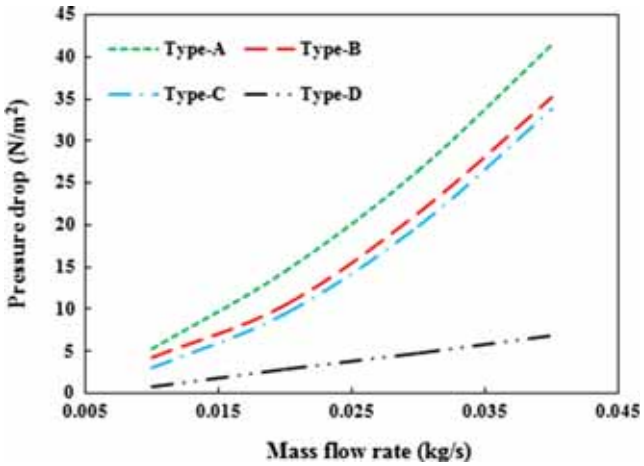

Figure 7. Variation of pressure drop with mass flow rate of air.

The highest exergy gain occurred through type-A solar air heater, while the lowest through type-D. The quality of available energy conversion into useful energy is higher in type-A solar air heater leading to higher exergy gain.

The effect of mass flow rate on the pressure drop through the type-A, type-B, type-C and type-D solar air heaters is presented in figure 7. It is clear from figure 7 that, for the four solar air heater considered, pressure drop increases with mass flow rate due to the increased velocity of the flowing air. It is obvious that the pressure drop through the type-A solar air heater is considerably higher than type-B, type-C and type-D solar air heaters due to increased friction while employing wire mesh, finned absorber plate and 180° close return bend. The pressure drop for type-B is slightly higher than type-C solar air heater. Pressure drop of type-D solar air heater slowly increases for all value of mass flow rate, compared to type-A, type-B and type-C solar air heaters. The maximum experimental pressure drop of type-D, type-C, type-B and type-A is 6.8 N/m^2, 33.7 N/m^2, 35.2 N/m^2 and 41.44 N/m^2 respectively at the experiment conducted with a mass flow rate of 0.04 kg/s. This is less than the results of El-khawajah *et al* [19] who employed multiple parallel layers of wire mesh with fins, reported a pressure drop of 84.5 N/m^2 at a mass flow rate of 0.042 kg/s. The results of single layer v-corrugated wire mesh in Type-A shows better thermal performance and minimum pressure drop.

5.2 *Effect of varied solar intensity*

The variation of temperature rise of air with solar intensity is shown in figure 8. Experimental results show that temperature rise of air increases with radiation intensity for all configurations due to an increase in the absorber plate temperature. Figure 8 clearly shows that the temperature rise of air for type-A is higher than type-B, type-C and type-D over the entire range of solar intensity considered.

The effect of solar intensity on energy efficiency of four types of solar air heaters is presented in figure 9. From the

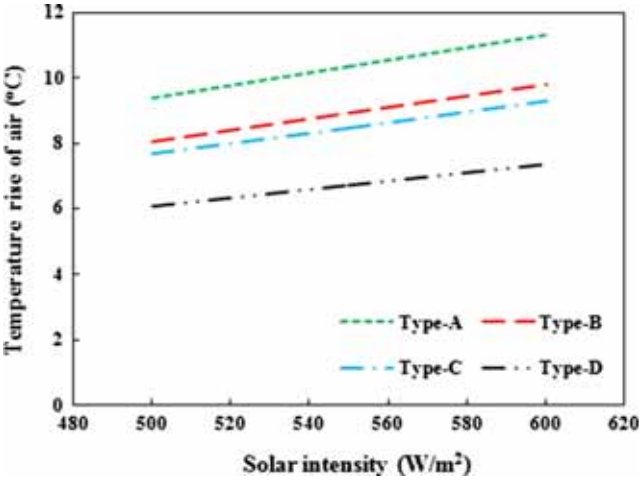

Figure 8. Variation of temperature rise of air with solar intensity.

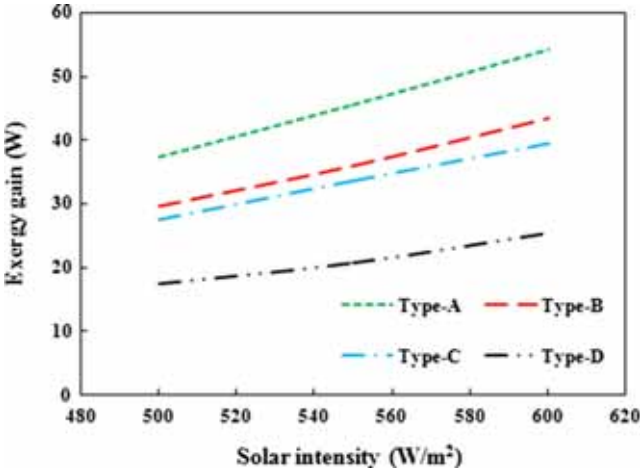

Figure 10. Variation of exergy gain with solar intensity.

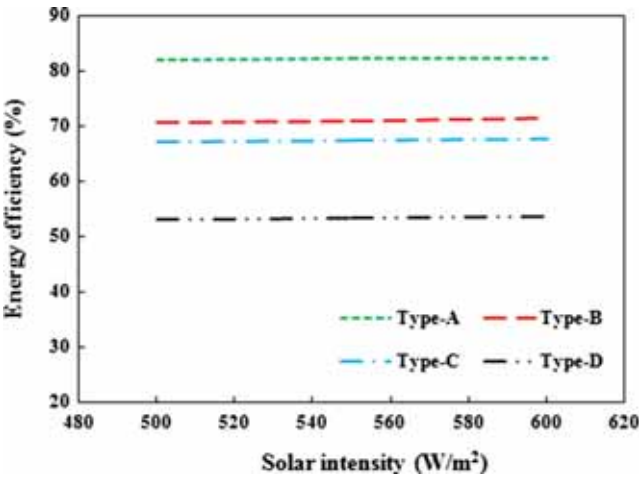

Figure 9. Variation of energy efficiency with solar intensity.

results, it is found that the type-A, type-B and type-C solar air heaters possess higher efficiency than type-D solar air heater. The type-A solar air heater performance is superior to type-B and type-C solar air heaters for all the values of solar intensity considered as the amount of solar energy absorbed and heat transfer area is higher. The results also show that solar intensity has little effect on the efficiencies of all four types of solar air heaters and is consistent with the results of Lin *et al* [22].

Figure 10 shows the plots of exergy gain of the type-A, type-B, type-C and type-D solar air heater as a function of solar intensity. It is clear from the results presented in figure 10 that the exergy gain increases with solar intensity for all configurations as the temperature difference between absorber plate and flowing air increases. It is found that type-A solar air heater has higher exergy gain than type-B type-C and type-D solar air heaters for all solar intensity (figure 10). The lowest exergy gain occurs in type-D solar air heater as only a little part of solar energy absorbed by the solar air heater is used for exergy gain.

6. Conclusion

An experimental study was conducted to evaluate the energy and exergy performances of four types of solar air heaters: v-corrugated wire mesh double pass solar air heater with longitudinal fins (type-A), finned plate double pass solar air heater with longitudinal fins (type-B), roughened plate double pass solar air heater with longitudinal fins (type-C), and conventional flat plate single pass solar air heater (type-D). All the solar air heaters were designed, constructed and tested under varied mass flow rate and solar intensity at steady state condition employing indoor experimental setup. The energy efficiency increases, while the temperature rise of air decreases with increasing mass flow rate of air. The maximum temperature rise of air obtained from this study is 26.28°C for type-A solar air heater at a mass flow rate of 0.01 kg/s. For type-A solar air heater, a maximum efficiency of 82.29% is obtained at a flow rate of 0.04 kg/s. The introduction of v-corrugated wire mesh layer in the second channel and longitudinal fins in the first channel of double pass mode creates turbulence intensity, enlargement in heat transfer area and increase in the path length. The temperature of absorber plate reduces owing to introduction of wire mesh and fins, decreases the heat loss to ambience and thereby, enhancing energy efficiency. The exergy gain decreases while pressure drop increases with mass flow rate of air. The type-A solar air heater exhibits better exergy gain and higher pressure drop than other conditions. In addition, the temperature rise of air and exergy gain increases with solar intensity (500–600 W/m^2), whereas energy efficiency is almost constant for all experimental conditions at similar mass flow rate. It is concluded from energy and exergy analysis that type-A solar air heater provides high quality and quantity energy gain than type-B, type-C and type-D solar air heaters. In addition, surface geometries are influential in enhancing the performance of solar air heater.

Nomenclature

A_c	surface area of the solar air heater (m^2)
c_p	specific heat of air at constant pressure (J/kg K)
I	solar intensity (W/m^2)
m	mass flow rate of air (kg/s)
ΔP	pressure drop across the solar air heater (N/m^2)
Q_f	useful energy gain of air (W)
T_a	ambient temperature (°C)
T_{fi}	inlet fluid temperature (°C)
T_{fm}	mean fluid temperature of inlet and outlet (°C)
T_{fo}	outlet fluid temperature (°C)

Greek letters

ρ	density of air (kg/m^3)
η	energy efficiency (%)

References

[1] Sopian K, Supranto Daud W R W, Othman M Y and Yatim B 1999 Thermal performance of the double pass solar collector with and without porous media. *Renew. Energy* 18: 557–564

[2] Ramadan M R I, El Sebaii A A, About Enein S and El-Bialy E 2007 Thermal performance of a packed bed double pass solar air heater. *Energy* 32: 1524–1535

[3] Omojaro A P and Aldabbagh L B Y 2010 Experimental performance of single and double pass solar air heater with fins and steel wire mesh as absorber. *Appl. Energy* 87: 3759–3765

[4] El-Sebaii A A, Aboul-Enein S, Ramadan M R I, Shalaby S M and Moharram B M 2011 Thermal performance investigation of double pass-finned plate solar air heater. *Appl. Energy* 88: 1727–1739

[5] Ozgen F, Esen M and Esen H 2009 Experimental investigation of thermal performance of a double flow solar air heater having aluminium cans. *Renew. Energy* 34: 2391–2398

[6] Karsli S 2007 Performance analysis of new design solar air collectors for drying applications. *Renew. Energy* 32: 1645–1660

[7] Gupta M K and Kaushik S C 2008 Exergetic performance evaluation and parametric studies of solar air heater. *Energy* 33: 1691–1702

[8] Esen H 2008 Experimental energy and exergy analysis of a double-flow solar air heater having different obstacles on absorber plates. *Build. Environ.* 43: 1046–1054

[9] Akpinar E K and Koçyiğit F 2010 Experimental investigation of thermal performance of solar air heater having different obstacle on absorber plates. *Int. Commun. Heat Mass Transfer* 37: 416–421

[10] BSI-BS 6757-1986 *British standard methods of test for thermal performance of solar collectors*. London: British Standard Institution

[11] JIS A 4112-1994 *Japanese industrial standard solar collectors*. Revised 1994-20-01, Japan: Japanese Standards Association

[12] Prasad B N 2013 Thermal performance of artificially roughened solar air heaters. *Sol. Energy* 91: 59–67

[13] Yang M, Wang P, Yang X and Shan M 2012 Experimental analysis on thermal performance of a solar air collector with a single pass. *Build. Environ.* 56: 361–369

[14] Mittal M K and Varshney L 2006 Optimal thermohydraulic performance of a wire mesh packed solar air heater. *Sol. Energy* 80: 1112–1120

[15] Sun W, Ji Jie and He Wei 2010 Influence of channel depth on the performance of solar air heaters. *Energy* 35: 4201–4207

[16] Holman J P 1994 *Experimental methods for engineers. 6th ed.* Singapore: McGraw-Hill Book Co

[17] Karim M A and Hawlader M N A 2006 Performance evaluation of a v-groove solar air collector for drying applications. *Appl. Therm. Eng.* 26: 121–130

[18] Mohamad A A 1997 High efficiency solar air heater. *Sol. Energy* 60(2): 71–76

[19] El-khawajah M F, Aldabbagh L B Y and Egelioglu F 2011 The effect of using transverse fins on a double pass flow solar air heater using wire mesh as an absorber. *Sol. Energy* 85: 1479–1487

[20] Prasad S B, Saini J S and Singh Krishna M 2009 Investigation of heat transfer and friction characteristics of packed bed solar air heater using wire mesh as packed materials. *Sol. Energy* 83: 773–783

[21] Dhiman P, Thakur N S and Chauhan S R 2012 Thermal and thermohydraulic performance of counter and parallel flow packed bed solar air heaters. *Renew. Energy* 46: 259–268

[22] Lin W, Gao W and Liu T 2006 A parametric study on the thermal performance of cross-corrugated solar air collectors. *Appl. Therm. Eng.* 26: 1043–1053